This document is confidential and is proprietary to the American Chemical Society and its authors. Do not copy or disclose without written permission. If you have received this item in error, notify the sender and delete all copies.

Chiral Measurement of Aspartate and Glutamate in Single Neurons by Large-volume Sample Stacking Capillary Electrophoresis

Journal:	*Analytical Chemistry*
Manuscript ID	ac-2017-034356.R1
Manuscript Type:	Article
Date Submitted by the Author:	n/a
Complete List of Authors:	Patel, Amit; University of Illinois at Urbana-Champaign, Chemistry Kawai, Takayuki; RIKEN, Quantitative Biology Center Wang, Liping; University of Illinois at Urbana-Champaign, Chemistry Rubakhin, Stanislav; University of Illinois, Beckman Institute Sweedler, Jonathan; University of Illinois at Urbana-Champ., Chemistry;

SCHOLARONE™
Manuscripts

Chiral Measurement of Aspartate and Glutamate in Single Neurons by Large-volume Sample Stacking Capillary Electrophoresis

Amit V. Patel, Takayuki Kawai, Liping Wang, Stanislav S. Rubakhin, and Jonathan V. Sweedler*

Department of Chemistry and Beckman Institute, University of Illinois at Urbana-Champaign, IL 61801, USA.

Keywords: D-amino acids, neurochemistry, single cell, chiral separations

ABSTRACT: D-Amino acids (D-AAs) are endogenous molecules found throughout the metazoan, the functions of which remain poorly understood. Measurements of low abundance and heterogeneously distributed D-AAs in complex biological samples, such as cells and multicellular structures of the central nervous system (CNS), require the implementation of sensitive and selective analytical approaches. In order to measure the D- and L- forms of aspartate and glutamate, we developed and applied a stacking chiral capillary electrophoresis (CE) with laser-induced fluorescence detection method. The achieved online analyte preconcentration led to a 480-fold enhancement of detection sensitivity relative to capillary zone electrophoresis, without impacting separation resolution or analysis time. Additionally, the effects of inorganic ions on sample preconcentration and CE separation were evaluated. The approach enabled the relative quantification of D-aspartate and D-glutamate in individual neurons mechanically isolated from the CNS of the sea slug *Aplysia californica*, a well-characterized neurobiological model. Levels of these structurally similar D-AAs were significantly different in subpopulations of cells collected from the investigated neuronal clusters.

Amino acids are an important class of small molecules that are critical for organismal function. Specifically, they are involved in cell-to-cell signaling and metabolism, and play a structural role as the building blocks of peptides and proteins.[1] With the exception of glycine, amino acids are chiral molecules and can be found in either the D- or L-form. In the context of higher animals, it was generally accepted that only the L-form was the physiologically relevant enantiomer, until this view was challenged by initial measurements of D-AAs in animal tissues.[2-4]

Following their discovery, numerous investigations of D-AAs have been carried out in invertebrate and vertebrate animal models. Notable non-mammalian examples include *Loligo vulgaris,*[3,5,6] *Pelophylax esculentus* (formerly *Rana esculenta*),[7-10] and *Aplysia californica*.[11,12] Research also been performed in mammals, such as the rat,[4,13-16] as well as in humans.[17-19] These studies have demonstrated the presence, and often the physiological importance, of different D-AAs.

Among these, D-serine (D-Ser) and D-aspartate (D-Asp) have been the most extensively studied. Functioning as a transmitter, D-Ser is an endogenous agonist for the N-methyl-D-aspartate (NMDA) receptor in different brain regions. Its misregulation is associated with schizophrenia and depression.[15,20-22] D-Asp exhibits all of the characteristics required for a neurotransmitter and/or neuromodulator.[6,11,23-26] Also, D-Asp has been associated with physiological processes such as neurogenesis,[27] reproduction,[9,19,25,28] and vision.[5] Despite the progress in understanding the endogenous roles of D-Ser and D-Asp, more work is required to better characterize their participation in numerous cell-to-cell signaling pathways, as well as their overall functional significance.

A number of other D-AAs have been detected in animals, but their biological functions remain poorly characterized.[29-31] For example, the functional roles of D-glutamate (D-Glu) remain enigmatic, despite its presence in various brain and peripheral tissues of the mouse,[31] in the brain, kidney, and liver of the rat,[32,33] the retina of multiple mollusks,[5] and throughout the nervous system of *Aplysia limacina*.[26] It appears that one limitation on the functional characterization of D-Glu relates to challenges associated with its measurement. It was recently reported that D-Glu was the only D-AA not found at detectable amounts in the mouse brain.[34]

Beyond its presence in biological tissues from a variety of animals, D-Glu may accumulate in rat synaptic vesicles, bind to NMDA receptors, and induce excitotoxicity.[35] Accumulation of D-Glu in the rat retina has also been reported.[36] Application of D-Glu was shown to cause muscle contraction in *Bombyx mori*,[37] as well as induce a rise in intracellular Ca^{2+} in muscle cells from *Pleurobrachia bachei* and *Bolinopsis infundibulum*.[38] Moreover, enzymes capable of catalyzing the degradation of D-Glu, D-glutamate cyclase, and D-aspartate oxidase (D-AspO), have been identified across the metazoan.[8,31,39-44] How is D-Glu synthesized? Although there are no well-characterized glutamate racemases, a recent study demonstrated glutamate racemase activity with known aspartate racemase enzymes from *Panaeus monodon* and *Crassostrea gigas*.[45] Interestingly, the murine glutamate-oxaloacetate transaminase 1-like 1 (GOT1L1), which was reported as an aspartate racemase, also exhibited dual racemase activity by synthesizing D-Glu in addition to D-Asp.[27] Follow-up work on rat and human homologs of GOT1L1 suggest it may not be the mammalian source of D-Asp.[46]

Measurement of D-AAs in animal tissues has largely been carried out via chiral liquid chromatography (LC) paired with detection by laser-induced fluorescence (LIF) or mass spectrometry (MS).[30,47-51] Though robust and successfully applied to the study of many different D-AAs in tissues from a broad range of animals, LC-based approaches are not as well suited for measuring volume-limited samples. Enzymatic biosensors have been shown to be useful for some such volume-limited measurements.[52] With regard to D-AA analyses at single cell and subcellular levels, these have been largely accomplished with chiral capillary electrophoresis (CE) paired with LIF detection.[11,53,54]

The limited progress on the characterization of a number of D-AAs in single cells is partly due to the analytical challenges of chiral single cell analyses. In addition to the difficulties associated with most chemical assays of biological

material, such as biofouling or system peak interference, analyses of D-AAs are further complicated by their low endogenous concentrations and heterogeneous distribution. Therefore, measurement of D-AAs at the single cell level requires the implementation of methodologies that can work with limited sample volumes, overcome sample matrix effects, and discriminate analytes on the basis of chirality with low limits of detection.

To address these challenges, we developed a variant of large-volume sample stacking (LVSS) chiral CE-LIF. There are a large number of characterization approaches for online preconcentration of analytes used in CE, often uniquely tailored for a given set of analytes. The wide variety of sample stacking approaches, as well as their mechanisms and applications, have been well reviewed.[55-58] The LVSS-CE-LIF approach described here afforded over two orders of magnitude signal enhancement and enabled analyses of D- and L-Asp, as well as D- and L-Glu, in single *A. californica* neurons. We observed differences in the amounts of the well characterized D-Asp, and the much less understood D-Glu.

Experimental Section

Materials and Chemicals. Chemicals were purchased from Sigma-Aldrich (St. Louis, MO) unless stated otherwise. Aqueous solutions were prepared with ultrapure deionized (DI) water from an ELGA Purelab Ultra water system (USFilter, Lowell, MA). Phosphate buffer saline (PBS) was purchased from Mediatech (Manassas, VA). Amino acids were stored as neat aqueous solutions at 14 °C. Naphthalene-2,3-dicarboxaldehyde (NDA) was purchased from Invitrogen (Carlsbad, CA). For the CE separations, 2-(N-morpholino)ethanesulfonic acid (MES), potassium bromide (KBr), and quaternary ammonium β-cyclodextrin (QAβCD) (CTD Holdings, Alachua, FL) were used. See the Supporting Information for experimental details relating to D-aspartate oxidase (D-AspO) cloning and purification. For D-Asp peak confirmation by enzymatic degradation via D-AspO, flavin adenine dinucleotide (FAD) and catalase (10,000–40,000 U/mg protein, 34 mg protein/mL suspension) from bovine liver were prepared in PBS. Homemade desalting tips were loaded with polymer slugs punched out from Empore polystyrene-divinylbenzene solid phase extraction (SPE) disks from 3M (St. Paul, MN).

Sample Preparation. *A. californica* were obtained from the *Aplysia* resource facility (University of Miami, Miami, FL), maintained in an aquarium with continuously circulating aerated and filtered sea water (Instant Ocean, Aquarium Systems Inc., Mentor, OH) at 14–15 °C until used. Animals for the single cell measurements weighed 125–200 g. For whole F-cluster measurements, animals weighed 5–20, 70–80 and 150–230 g for the juvenile, small adult, and large adult samples, respectively. Animals were anesthetized by injection of isotonic $MgCl_2$ (~30 to ~50% of body weight) into the body cavity. The cerebral ganglia were dissected and placed in artificial sea water (ASW) containing (in mM): 460 NaCl, 10 KCl, 10 $CaCl_2$, 22 $MgCl_2$, 6 $MgSO_4$, and 10 HEPES (pH 7.8), or in ASW-antibiotic solution (ASW supplemented with 100 units/mL penicillin G, 100 μg/mL streptomycin, and 100 μg/mL gentamicin, pH 7.8). To facilitate mechanical isolation of cellular clusters and individual neurons, the ganglion sheath was digested enzymatically by incubation in 1% protease (Type IX: Bacterial) ASW-antibiotic solution at 34 °C for 40–90 min, depending on animal size and season. Isolated ganglia, cellular clusters, and cells were washed in fresh ASW.

Each isolated cell was separately placed in 100 μL of methanol, sonicated for 10 min at 20 °C, and then centrifuged at 9000 *g* for 5 min. Thereafter, the supernatant was collected and then dried with a Savant SpeedVac concentrator (Thermo, Milford, MA). All samples were reconstituted in DI water.

Sample Derivatization and Desalting. Derivatization procedures for the standards and samples for LIF detection were accomplished by mixing the aqueous standard mixture or sample with NDA (20 mM in acetonitrile (ACN)) and potassium cyanide (KCN) (saturated in ACN, 20 °C) in a 1:1:2 ratio. Mixing was achieved with pipetting and the reaction was allowed to proceed for one hour in the dark at 20–24 °C. SAFETY NOTE: our NDA reaction protocol involves the use of unbuffered KCN and should be carried out in a fume hood while following safety procedures to minimize risk of cyanide exposure. Alternative reaction protocols can also be considered.

Following derivatization, each reaction mixture was dried under vacuum, reconstituted in DI water, and desalted by homemade centrifuge extraction tips.[59] In brief, SPE columns were constructed by loading 0.7–0.8 mg of polystyrene-divinylbenzene into a 200 μL pipette tip. Next, the SPE polymer bed material was activated with pure ACN, conditioned with water, loaded with a reaction mixture in minimum volume, desalted with 10 μL water, and analytes eluted with 20 μL pure ACN. Finally, each eluted, desalted sample was quickly dried under vacuum and reconstituted in DI water.

In order to confirm the presence of D-Asp, we treated some samples with D-AspO; thus, several amino acid standards and single cell extracts were mixed with D-AspO (4.6 mg/mL), FAD (5 mM), and catalase (68 μg/mL) in a 1:0.6:1:1 volume ratio. Next, the mixture was incubated in a water bath at 37 °C for 5.75 h. Each enzyme-treated sample was dried and reconstituted in 1 μL of water prior to derivatization, desalting, and analysis by CE-LIF.

Capillary Zone Electrophoresis (CZE)-LIF. Separations were performed with a PA 800 plus Pharmaceutical Analysis System with LIF detection (AB SCIEX, Framingham, MA). This system was coupled to an external diode laser (56ICS426, Melles Griot, Carlsbad, CA) with a fiber optic cable (OZ Optics, Ottawa, ON, Canada). The laser was operated at 3 mW with an emission wavelength of 440 ± 8 nm. The LIF detection module was modified with a 490 ± 15 nm band-pass filter (Omega Optical, Brattleboro, VT) to permit only the fluorescence emission band to reach the photomultiplier tube.

LVSS-CE-LIF. Buffer solutions were prepared in DI water to avoid impurities and minimize conductivity. We prepared 250 mL of 280 mM MES buffer (pH 6.00) by dissolving 14.6633 g of MES hydrate (4.7% H_2O) in 200 mL of DI water, adjusting pH with 1.0 M NaOH, and then diluting to volume with DI water. A 10% (w/v) QAβCD solution was prepared by dissolving 0.0790 g of QAβCD in 0.790 mL of DI water. Additionally, we prepared 200 mM KBr by dissolving 2.39 g of KBr into 100 mL of DI water. The separation buffer with final concentrations of 60 mM MES (pH 6), 10 mM KBr, and 110 ppm QAβCD, was prepared daily by mixing appropriate amounts of each component and DI water. Prior to use, buff-

ers were degassed by sonication. Bare fused-silica capillaries (Polymicro Technologies, Phoenix, AZ) were used for all separations. The total/effective lengths of the capillaries were 50/40 cm, with inner/outer diameters of 50/360 μm. All capillaries were treated with 0.1 M NaOH for 30 min prior to initial use. Further, all capillaries were sequentially rinsed with 0.1 M NaOH, DI water, and separation buffer for one min prior to each analysis. The separation buffer was replenished prior to each separation. Whole capillary volume sample injection was performed hydrodynamically with a pressure of 20.0 psi for one min. For both the LVSS and CZE separation methods, the voltage and temperature were -26 kV and 18 °C respectively. OriginPro 2015 software (Origin Lab Corp., Northampton, MA) was used for data analysis.

Results and Discussion

Comparison of CZE and LVSS-CE Separation Performance. An LVSS-CE-LIF technique was developed for the chiral analysis of D- and L-Asp, and D- and L-Glu. LVSS, also referred to as large-volume sample stacking with an electroosmotic flow pump (LVSEP), leverages conductivity differences between the sample and background electrolyte (BGE), as well as the reversal of the direction of electroosmotic flow by BGE additives for sample stacking. The general principles of the stacking process, as well as information on other LVSEP methods and applications, have been well described in the review by Kitagawa and coworkers.[60]

In this variant of LVSS-CE-LIF, the entire capillary is filled with low conductivity sample. Prior to separation, analytes are compressed to a narrow band by field-enhanced stacking. Due to large sample loading relative to CZE-LIF, the signal for each of the stacked analytes increases proportionally, as opposed to being a function of electrophoretic mobility. This attribute of even signal gain is important in analyses where molecules of interest migrate near high mobility system peaks.

A signal enhancement of 480 ± 12-fold ($\bar{x}$ ± SD) was achieved using the LVSS-CE-LIF chiral analysis method, as determined by comparing triplicate inter-day measurements against those from CZE under equivalent capillary and buffer conditions (**Figure 1 A, B**). The relative standard deviations of the peak areas and migration times were comparable between the LVSS and CZE analyses (**Table 1**). Additionally, as seen in **Figure 1C**, the current profiles for both LVSS and CZE were stable and repeatable. The initial lack of current in the LVSS-CE current profile corresponds to the sample stacking process. Following sample preconcentration, the amplitude of the LVSS-CE-associated current is 97% of CZE current under identical separation conditions. The difference in the current amplitudes for the two methods depends on the extent of surface coverage with QAβCD, which dynamically coats the capillary walls during the sample stacking process.

Once the method's repeatability was established, we confirmed its ability to resolve the analyte signals from system peaks. **Figure 1D** shows a representative electropherogram from a single neuron from the F-cluster of *Aplysia*. D-Glu was not observed in most of the analyzed neurons. However, when present, the developed LVSS-CE method well resolves D-Glu from system peaks, enabling detection at trace levels (**Figure 2A**). Our results demonstrate that the LVSS-CE-LIF method is well suited for analyses of D- and L-Asp, as well as D- and L-Glu, in single neurons. Analyte peaks were identified by migration time, shape, and standard addition

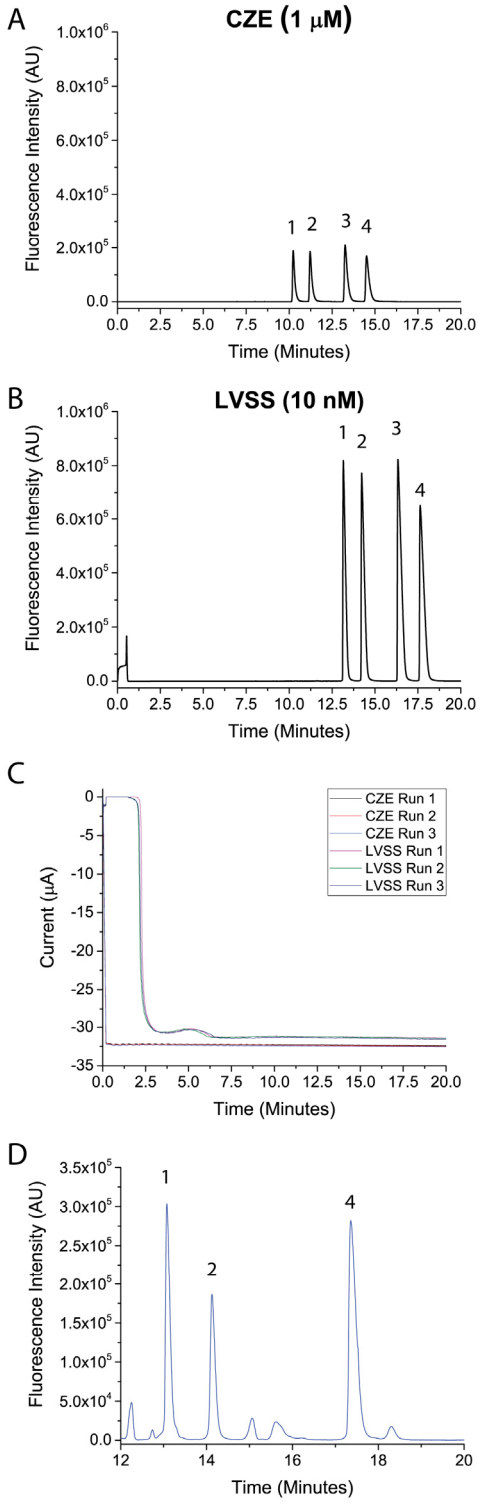

Figure 1. Comparison of CZE-LIF and LVSS-CE-LIF performance. (A) CZE-LIF electropherogram from the analysis of D- and L-Asp, and D- and L-Glu by CZE. (B) CZE-LIF electropherogram from the analysis of D- and L-Asp, and D- and L-Glu by LVSS. (C) Current profiles for CZE and LVSS separations (n=3 for each method). (D) Representative electropherogram from the analysis of a single neuron from the F-cluster of the cerebral ganglion. Peaks in the electropherograms: (1) L-Asp, (2) D-Asp, (3) D-Glu, and (4) L-Glu.

Table 1. The intra-day and inter-day repeatability of the CZE and LVSS methods. Relative standard deviations for peak areas and migration times for D- and L-aspartate, AND D- and L-glutamate (n = 3) are presented.

	Peak Area Relative Standard Deviation (%)				Migration Time Relative Standard Deviation (%)			
	Capillary Zone Electrophoresis		Large-Volume Sample Stacking		Capillary Zone Electrophoresis		Large-Volume Sample Stacking	
Analyte	Intra-Day	Inter-Day	Intra-Day	Inter-Day	Intra-Day	Inter-Day	Intra-Day	Inter-Day
L-Aspartate	4.4	11.8	6.2	11.2	0.5	0.7	0.8	1.3
D-Aspartate	4.3	11.5	6.4	11.0	0.5	0.8	0.9	1.4
L-Glutamate	4.6	12.0	7.7	12.0	0.7	1.0	1.0	1.8
D-Glutamate	4.6	11.8	7.5	12.9	0.7	1.1	1.1	2.0

experiments. As shown in **Figure 2B**, the D-Asp peak identifications were also confirmed with enzymatic treatment of single cell extracts by the degradative enzyme D-AspO.

Effects of Inorganic Ions on Method Performance. It is often the case that single cell samples contain inorganic ions that can interfere with chemical measurements. These ions include those endogenous to the biological material itself, but also are often sourced from the solutions used for sample preparation (e.g., cell isolation or culture media). These solutions are frequently comprised of millimolar quantities of inorganic ions, notably Na^+ and Cl^-. For this reason, we investigated the impact of both ions on the performance of the LVSS-CE-LIF method used here.

In this experiment, 10 nM standards of D- and L-Asp, and D- and L-Glu, were analyzed by LVSS-CE-LIF with increasing amounts of NaCl added. The impact of NaCl levels on the current profile is also shown in **Figure S1A**. Control LVSS-CE-LIF measurements of 10 nM standards, and CZE-LIF detections of 1 μM standards in the absence of the inorganic ions, are shown in **Figure S1B**. LVSS-CE-LIF analyses were able to tolerate the presence of up to 1 mM NaCl without detriment to signal intensity, migration time, and current profile. More substantial deteriorations of signal intensity and peak shape were observable with 10 and 100 mM NaCl, where 100 mM NaCl induced shifts in migration time. However, even under these conditions, LVSS-CE-LIF produced stronger signals for the analyzed standards as compared to CZE-LIF analyses of the same standards at two orders of magnitude greater concentrations (**Figure S1B**). The salt tolerance of this method is greater than similar LVSS approaches, typically in the low-mid μM range.[61] The resulting signal enhancement and salt tolerance are attributed to a "double stacking" mechanism, the combination of field-enhanced and sweeping stacking, as depicted in **Figure 3**. Substantial changes in the current profiles during stacking, and the analyte separation itself, were also observed with 10 and 100 mM NaCl (**Figure S2**).

Although our LVSS-CE-LIF method tolerates high levels of salt, the observed effects of the presence of inorganic ions on method performance prompted the inclusion of a desalting step to our analytical protocol. Desalting ensures that all samples are devoid of salts as opposed to containing unknown and variable amounts, affording more consistent migrations times and signal enhancement. To this end, we developed a homemade SPE approach by packing a 200 μL pipette tip with polystyrene-divinylbenzene. This bed material was selected because it was anticipated to interact strongly with the tagged amino acids, which undergo substantial increases in hydrophobicity upon derivatization. The hydrophobic interactions between the cyanobenz[f]isoindole-amino acids and the SPE bed material enable analyte retention and sample desalting. In order to evaluate the developed SPE approach, a stock solution containing 100 μM standards was diluted to achieve 10 nM levels, with reduced concentrations of other compounds present in the derivatization mix-

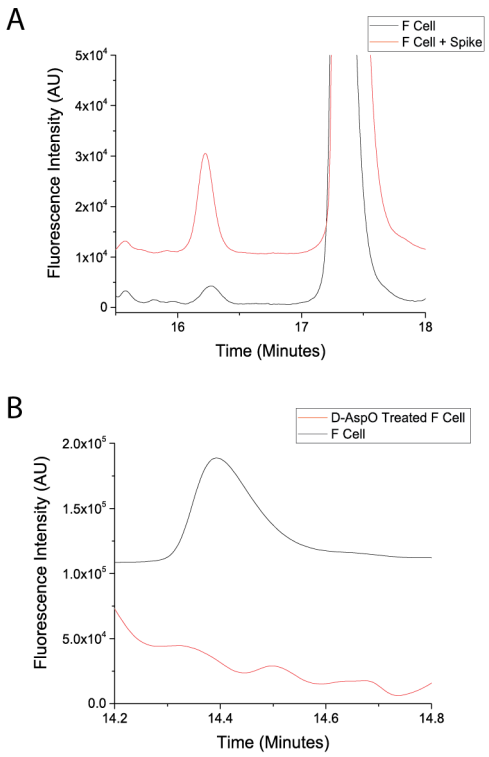

Figure 2. Peak identification by standard addition or enzymatic degradation. (A) Electropherogram from the LVSS-CE-LIF analysis of a single neuron from the F-cluster of the cerebral ganglion with (Red) and without (Black) 100 pM D-Glu spike. (B) Electropherogram from the LVSS-CE-LIF analysis of a single neuron from the F-cluster of the cerebral ganglion with (Red) and without (Black) enzymatic treatment by D-AspO. The peak corresponding to D-Asp is degraded with enzymatic treatment.

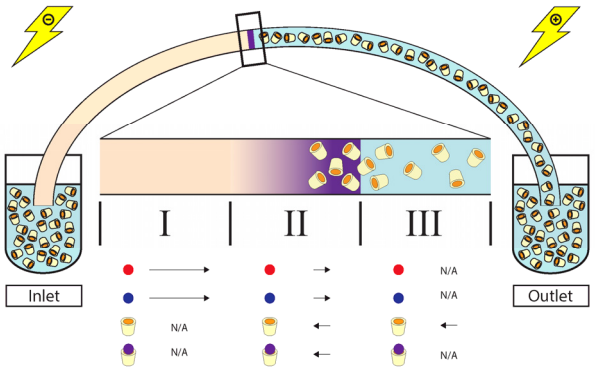

Figure 3. Depiction of the sample stacking process in the LVSS variant. The D-AAs (Red) and L-AAs (Blue) are stacked together (shown as Purple); the chiral separation initiates once Regions I and II are excreted from the capillary inlet by electroosmotic flow. **Region I:** This region of the capillary contains low conductivity sample matrix (devoid of analyte as the acidic amino acids have migrated to Region II). **Region II:** This is the boundary between the low conductivity sample and high conductivity BGE. Upon reaching this boundary, analytes are exposed to a lower separation potential as well as sweeping towards the inlet when complexed with the cationic cyclodextrin additive. **Region III:** High conductivity BGE containing the chiral additive QAβCD.

ture. SPE-treated and control (untreated) standards containing 10 nM of DL-Asp and DL-Glu were analyzed in triplicate. The current traces for the LVSS-CE-LIF analyses of SPE-treated and diluted samples overlay well, and match the current profile observed from the traces measured in the absence of added inorganic ions (**Figure S3**). The percent recovery ($\bar{x}$ ± SD), calculated for each enantiomer individually as the ratio of SPE and diluted standard peak areas from triplicate measurements, were 63 ± 5% for D/L-Asp, and 74 ± 6% for D/L-Glu. Thus, the overall signal enhancement from the developed approach remained greater than two orders of magnitude in spite of losses from the desalting step.

LVSS-CE-LIF Analysis of Single Neurons. To demonstrate the applicability of the developed approach for quantification, calibration plots over the range of relevant concentrations were constructed. The determined limits of detection were sub-pM, and R^2 values were greater than 0.996 for each amino acid (**Figure S4**).

The contribution of analytes present in the extracellular media collected during single cell sample preparation was tested. We collected and analyzed 1 µL of media surrounding the neuron of interest, which is notably larger than what is typically transferred alongside a single cell during sampling. Even with this excessive volume, signals corresponding to < 5 pmol L-Asp and L-Glu were detected, with no signals of D-Asp and D-Glu observed (data not shown). Therefore, no significant influence from the extracellular media on the results of single cell analysis is expected.

Due to the irregular shape and complex morphology of the studied cells, volume determination by microscopy is complicated and inexact. For this reason, relative quantification was performed where % of D-Glu (and % D-Asp) is related to the total (L + D) Glu (and L + D Asp), where the variance of % D-AA is driven by the variance of the D-AA levels and not the less variable and consistently high concentrations of

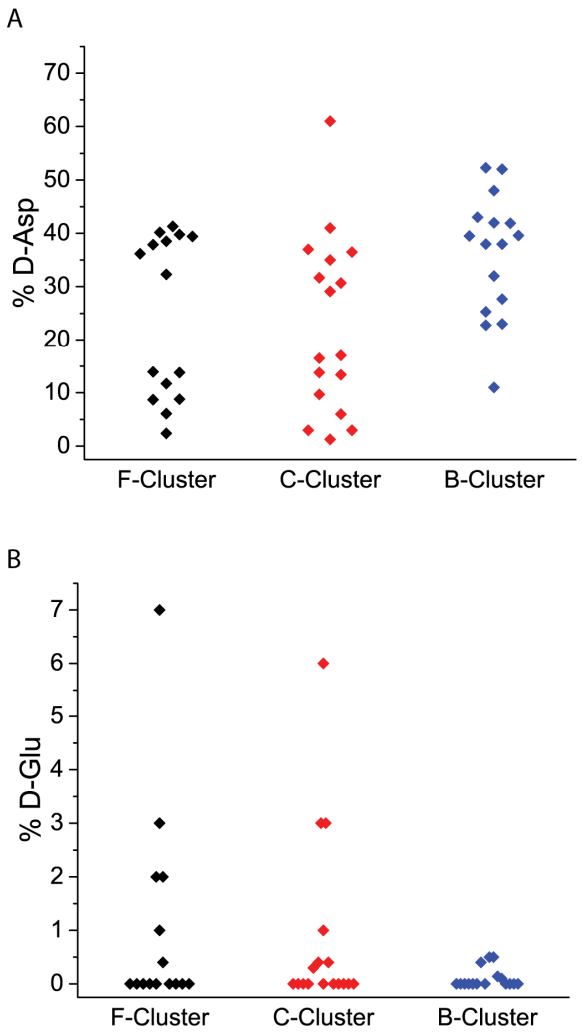

Figure 4. Scatterplots of (A) % D-Asp and (B) % D-Glu measured in individual neurons from the F-, C-, and B-clusters of the cerebral ganglion; each point corresponds to a single cell. Number of single neurons analyzed per cluster, sample size (n): F-cluster = 15, C-cluster = 17, B-cluster = 16.

the L-forms. Multiple neurons from the F-, C- and B-clusters of the *Aplysia* cerebral ganglion were measured individually (**Figure 4**). Although all three of these clusters were shown to stain positively for DAR1 protein, a large range of % D-Asp contents was apparent (**Figure 4A**). The % D-Glu was much lower than % D-Asp in all studied cells. Interesting, unlike D-Asp, D-Glu-containing neurons were found only in the F- and C-clusters (**Figure 4B**). Additionally, as can be seen in **Figure 4**, neuronal sub-populations are observable within the datasets.

None of the analyzed neurons demonstrated % D-Asp outside of the inner fence values (**Figure S5A**). Analysis of entire F-clusters from animals of varied sizes, and thereby varied ages, found an anticipated age/size-dependent increase in % D-Asp (**Figure S6**). With regard to % D-Glu, several neurons fell outside the inner fence values (**Figure S5B**). Additionally, the mode for % D-Glu datasets for each cluster equals 0. Taken together, the identified "outlier" cells are neurons with notably different D-AA content from the others

in the dataset — in this case, the rare D-Glu containing neurons.

No correlation between the relative levels of the two D-AAs is apparent (**Figure 5**). This lack of correlation suggests that individual cell-specific accumulation of D-AAs can be involved in the observed phenomenon. Also, different enzymes may be involved in the synthesis of these structurally similar D-AAs. As an example, the presence of another enzyme capable of synthesizing D-AAs in *A. californica*, DAR1L, was recently shown.[45] However, the cellular distribution of DAR1L in the *Aplysia* CNS, as well as the possible existence and localization of other enzymes that may play a role in the synthesis and degradation of D-AAs, remain unknown.

How confident are our assignments? The LVSS-CE-LIF approach was validated with measurements of D-Asp in single *Aplysia* neurons known to express the enzyme DAR1. Following peak identification by migration time and standard addition, enzymatic digestion by D-AspO was used to demonstrate that the measured values indeed correspond to D-Asp, and not a co-migrating peak. With regard to D-Glu, challenges associated with enzymatic treatment of this low-abundance analyte in single cell samples, combined with this enzyme's lower efficiency in eliminating D-Glu, prevented us from confirming the peak identity via an enzymatic test. Thus, our identification of D-Glu was based on migration time, peak shape, and standard addition. Although peak identifications as done here for D-Glu and by others for various D-AAs[34] can be effective, they should be considered tentative.

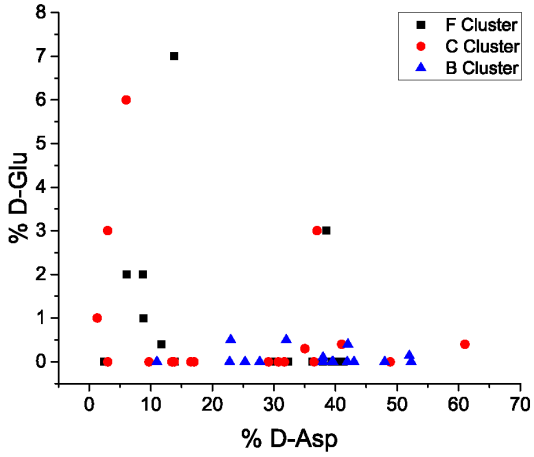

Figure 5. Scatter plot of % D-Asp and % D-Glu determined for multiple individual neurons isolated from three different clusters of the cerebral ganglion. Each point corresponds to data collected from a single neuron. Sample size (n): F-cluster neurons = 15, C-cluster neurons = 17, B-cluster neurons = 16.

Conclusions

Neurochemistry tends to be conserved across the metazoan and the presence of D-AAs appears to follow this trend. D-Glu has been measured at 0.5% in the rat brain,[32] and immunocytochemical staining identified the sparse presence of D-Glu-containing cells (< 1%) in several regions of the rat brain.[33] Our data support the idea of sparse D-Glu presence in the CNS, making it an intriguing and important molecule to understand. The ability to carry out single cell studies is important when analyzing chemical species such as D-Glu, which are heterogeneously distributed between cells in the targeted biological structure. The herein described variant of LVSS-CE-LIF enables analyses of both enantiomeric forms of aspartate and glutamate in single neurons, with an over two orders of magnitude sensitivity enhancement compared to the traditional CZE-LIF approach. The efficacy of the technique was validated by analyses of D-Asp and D-Glu in individual neurons from defined clusters of the cerebral ganglion of *A. californica*. Significant differences in relative contents of D-Asp and D-Glu between studied cells of differing origin were readily identified. Based on a rough estimation of cell size and signal intensity, the levels measured in these cells correspond to low µM concentrations of D-Glu and high µM to low mM concentrations of D- and L-Asp, as well as L-Glu. The ability to measure D-Glu in single neurons will aid efforts in characterizing this enigmatic D-AA, which exhibits low abundance and a heterogeneous distribution.

Robust D-AA measurements make use of ancillary approaches such as analyte-specific enzymatic treatment as shown here, or some excellent examples from the literature.[26,29,46,54] Employing multiple analytical techniques to measure the same analytes from the same samples can provide greater confidence for such measurements.[62] Unfortunately, these ancillary approaches are not always effective for single cell measurements. Our group and others have worked on single cell CE–MS,[63-71] but these approaches need to be adapted for chiral measurement. Until then, the results reported here, and similar studies lacking ancillary confirmation for their analytes, are unconfirmed and require follow-up studies.

Future work will involve more in-depth single cell analyses in *Aplysia* and other models, including smaller mammalian brain cells, for the purposes of identifying neurons that utilize D-Glu for signaling, and for follow-up studies aimed at discovering enzyme(s) involved in its biosynthesis.

ASSOCIATED CONTENT

Supporting Information

Details describing the cloning and purification of D-AspO, and Supporting Figures S1–S6, as noted in the text (PDF). The Supporting Information is available free of charge on the ACS Publications website at http://pubs.acs.org.

AUTHOR INFORMATION

Corresponding Author

*Phone: 217-244-7359. Fax: 217-265-6290. E-mail: jsweedle@illinois.edu

Notes

The authors declare no competing financial interest.

Author Contributions

The manuscript was written with contributions from all authors. All authors have given approval to the final version of the manuscript.

ACKNOWLEDGMENTS

We thank Dr. Nobutoshi Ota for enzyme production and for discussions regarding enzymatic treatments. We would like to also thank the National Resource for Aplysia (Miami, FL), funded by PHS grant P40 OD010952, for sourcing the animals. This project was supported by Award No. CHE-16-067915 from the National Science Foundation and P30 018310 from the National Institute on Drug Abuse. A.V.P. acknowledges funding from the Eastman Summer Fellowship.

REFERENCES

(1) Meijer, A. J.; Dubbelhuis, P. F. *Biochem. Biophys. Res. Commun.* **2004**, *313*, 397-403.
(2) Corrigan, J. J. *Science* **1969**, *164*, 142-149.
(3) D'Aniello, A.; Giuditta, A. *J. Neurochem.* **1978**, *31*, 1107-1108.
(4) Hashimoto, A.; Nishikawa, T.; Hayashi, T.; Fujii, N.; Harada, K.; Oka, T.; Takahashi, K. *FEBS Lett.* **1992**, *296*.
(5) D'Aniello, S.; Spinelli, P.; Ferrandino, G.; Peterson, K.; Tsesarskia, M.; Fisher, G.; D'Aniello, A. *Biochem. J.* **2005**, *386*, 331-340.
(6) D'Aniello, S.; Somorjai, I.; Garcia-Fernandez, J.; Topo, E.; D'Aniello, A. *FASEB J.* **2010**, *25*, 1014-1027.
(7) Di Fiore, M. M.; Assisi, L.; Botte, V.; D'Aniello, A. *J. Endocrinol.* **1998**, *157*, 199-207.
(8) Di Giovanni, M.; Burrone, L.; Chieffi Baccari, G.; Topo, E.; Santillo, A. *J. Exp. Zool. A Ecol. Genet. Physiol.* **2010**, *313A*, 137-143.
(9) Raucci, F.; Di Fiore, M. M. *J. Chromatogr. B* **2011**, *879*, 3268-3276.
(10) Raucci, F.; Santillo, A.; D'Aniello, A.; Chieffi, P.; Baccari, G. C. *J. Cell. Physiol.* **2005**, *204*, 445-454.
(11) Miao, H.; Rubakhin, S. S.; Scanlan, C. R.; Wang, L.; Sweedler, J. V. *J. Neurochem.* **2006**, *97*, 595-606.
(12) Scanlan, C.; Shi, T.; Hatcher, N. G.; Rubakhin, S. S.; Sweedler, J. V. *J. Neurochem.* **2010**, *115*, 1234-1244.
(13) Imai, K.; Fukushima, T.; Hagiwara, K.; Santa, T. *Biomed. Chromatogr.* **1995**, *9*, 106-109.
(14) Monteforte, R.; Santillo, A.; Giovanni, M.; D'Aniello, A.; Maro, A.; Chieffi Baccari, G. *Amino Acids* **2008**, *37*, 653-664.
(15) Schell, M. J.; Brady Jr., R. O.; Molliver, M. E.; Snyder, S. H. *J. Neurosci.* **1997**, *17*, 1604-1615.
(16) Wang, H.; Wolosker, H.; Pevsner, J.; Snyder, S. H.; Selkoe, D. J. *J. Endocrinol.* **2000**, *167*, 247-252.
(17) Dunlop, D. S.; Neidle, A.; McHale, D.; Dunlop, D. M.; Lajtha, A. *Biochem. Biophys. Res. Commun.* **1986**, *141*, 27-32.
(18) Fuchs, S. A.; Dorland, L.; De Sain-Van Der Velden, M. G.; Hendriks, M.; Klomp, L. W. J.; Berger, R.; De Koning, T. J. *Ann. Neurol.* **2006**, *60*, 476-480.
(19) Topo, E.; Soricelli, A.; D'Aniello, A.; Ronsini, S.; D'Aniello, G. *Reprod. Biol. Endocrinol.* **2009**, *7*, 120.
(20) Fossat, P.; Turpin, F. R.; Sacchi, S.; Dulong, J.; Shi, T.; Rivet, J. M.; Sweedler, J. V.; Pollegioni, L.; Millan, M. J.; Oliet, S. H. R.; Mothet, J. P. *Cereb. Cortex* **2011**, *22*, 595-606.
(21) Oliet, S. H. R.; Mothet, J. P. *Glia* **2006**, *54*, 726-737.
(22) Van Horn, M. R.; Sild, M.; Ruthazer, E. S. *Front. Cell. Neurosci.* **2013**, *7*, 1-13.
(23) D'Aniello, A. *Brain Res. Rev.* **2007**, *53*, 215-234.
(24) Ota, N.; Shi, T.; Sweedler, J. V. *Amino Acids* **2012**, *43*, 1873-1886.
(25) Santillo, A.; Pinelli, C.; Burrone, L.; Chieffi Baccari, G.; Di Fiore, M. M. *Gen. Comp. Endocrinol.* **2013**, *181*, 72-76.
(26) Spinelli, P.; Brown, E. R.; Ferrandino, G.; Branno, M.; Montarolo, P. G.; D'Aniello, E.; Rastogi, R. K.; D'Aniello, B.; Baccari, G. C.; Fisher, G.; D'Aniello, A. *J. Cell. Physiol.* **2006**, *206*, 672-681.
(27) Kim, P. M.; Duan, X.; Huang, A. S.; Liu, C. Y.; Ming, G. l.; Song, H.; Snyder, S. H. *Proc. Natl. Acad. Sci. U. S. A.* **2010**, *107*, 3175-3179.
(28) Raucci, F.; Di Fiore, M. M. *J. Histochem. Cytochem.* **2009**, *58*, 157-171.
(29) Hamase, K.; Inoue, T.; Morikawa, A.; Konno, R.; Zaitsu, K. *Anal. Biochem.* **2001**, *298*, 253-258.
(30) Hamase, K.; Morikawa, A.; Ohgusu, T.; Lindner, W.; Zaitsu, K. *J. Chromatogr.* **2007**, *1143*, 105-111.
(31) Han, H.; Miyoshi, Y.; Koga, R.; Mita, M.; Konno, R.; Hamase, K. *J. Pharm. Biomed. Anal.* **2015**, *116*, 47-52.
(32) Kera, Y.; Aoyama, H.; Matsumura, H.; Hasegawa, A.; Nagasaki, H.; Yamada, R. *Biochim. Biophys. Acta* **1995**, *1243*, 282-286.
(33) Mangas, A.; Coveñas, R.; Bodet, D.; Geffard, M.; Aguilar, L. A.; Yajeya, J. *Neuroscience* **2007**, *144*, 654-664.
(34) Weatherly, C. A.; Du, S.; Parpia, C.; Santos, P. T.; Hartman, A. L.; Armstrong, D. W. *ACS Chem. Neurosci.* **2017**, *8*, 1251-1261.
(35) Pan, Z. Z.; Tong, G.; Jahr, C. E. *Neuron* **1993**, *11*, 85-91.
(36) Pow, D. V.; Crook, D. K. *Neuroscience* **1996**, *70*, 295-302.
(37) Sekimizu, K. *J. Biochem.* **2005**, *137*, 199-203.
(38) Moroz, L. L.; Kocot, K. M.; Citarella, M. R.; Dosung, S.; Norekian, T. P.; Povolotskaya, I. S.; Grigorenko, A. P.; Dailey, C.; Berezikov, E.; Buckley, K. M.; Ptitsyn, A.; Reshetov, D.; Mukherjee, K.; Moroz, T. P.; Bobkova, Y.; Yu, F.; Kapitonov, V. V.; Jurka, J.; Bobkov, Y. V.; Swore, J. J., et al. *Nature* **2014**, *510*, 109-114.
(39) D'Aniello, A.; D'Onofrio, G.; Pischetola, M.; D'Aniello, G.; Vetere, A.; Petrucelli, L.; Fisher, G. *J. Biol. Chem.* **1993**, *25*, 26941-26949.
(40) Errico, F.; Pirro, M. T.; Affuso, A.; Spinelli, P.; De Felice, M.; D'Aniello, A.; Di Lauro, R. *Gene* **2006**, *374*, 50-57.
(41) Katane, M.; Homma, H. *Chem. Biodivers.* **2010**, *7*, 1435-1449.
(42) Katane, M.; Saitoh, Y.; Seida, Y.; Sekine, M.; Furuchi, T.; Homma, H. *Chem. Biodivers.* **2010**, *7*, 1424-1434.
(43) Yamamoto, A.; Tanaka, H.; Ishida, T.; Horiike, K. *J. Neuroendocrinol.* **2010**, *22*, 1165-1172.
(44) Ariyoshi, M.; Katane, M.; Hamase, K.; Miyoshi, Y.; Nakane, M.; Hoshino, A.; Okawa, Y.; Mita, Y.; Kaimoto, S.; Uchihashi, M.; Fukai, K.; Ono, K.; Tateishi, S.; Hato, D.; Yamanaka, R.; Honda, S.; Fushimura, Y.; Iwai-Kanai, E.; Ishihara, N.; Mita, M., et al. *Sci. Rep.* **2017**, *7*, 43911.
(45) Uda, K.; Abe, K.; Dehara, Y.; Mizobata, K.; Sogawa, N.; Akagi, Y.; Saigan, M.; Radkov, A. D.; Moe, L. A. *Amino Acids* **2015**, *48*, 387-402.
(46) Matsuda, S.; Katane, M.; Maeda, K.; Kaneko, Y.; Saitoh, Y.; Miyamoto, T.; Sekine, M.; Homma, H. *Amino Acids* **2015**, *47*, 975-985.
(47) Song, Y.; Feng, Y.; LeBlanc, M. H.; Zhao, S.; Liu, Y. *Anal. Chem.* **2006**, *78*, 8121-8128.
(48) Song, Y.; Feng, Y.; Lu, X.; Zhao, S.; Liu, C.-W.; Liu, Y.-M. *Neurosci. Lett.* **2008**, *445*, 53-57.
(49) Kato, S.; Masuda, Y.; Konishi, M.; Oikawa, T. *J. Pharm. Biomed. Anal.* **2015**, *116*, 101-104.
(50) Karakawa, S.; Shimbo, K.; Yamada, N.; Mizukoshi, T.; Miyano, H.; Mita, M.; Lindner, W.; Hamase, K. *J. Pharm. Biomed. Anal.* **2015**, *115*, 123-129.
(51) Morikawa, A.; Hamase, K.; Inoue, T.; Konno, R.; Niwa, A.; Zaitsu, K. *J. Chromatogr. B Biomed. Sci. Appl.* **2001**, *757*, 119-125.
(52) Polcari, D.; Kwan, A.; Van Horn, M. R.; Danis, L.; Pollegioni, L.; Ruthazer, E. S.; Mauzeroll, J. *Anal. Chem.* **2014**, *86*, 3501-3507.

(53) Miao, H.; Rubhakin, S. S.; Sweedler, J. V. *Anal. Chem.* **2005**, *77*, 7190-7194.
(54) Ota, N.; Rubakhin, S. S.; Sweedler, J. V. *Biochem. Biophys. Res. Commun.* **2014**, *447*, 328-333.
(55) Chen, Y.; Lü, W.; Chen, X.; Teng, M. *Cent. Eur. J. Chem.* **2012**, *10*, 611-638.
(56) Simpson, S. L.; Quirino, J. P.; Terabe, S. *J. Chromatogr.* **2008**, *1184*, 504-541.
(57) Aranas, A. T.; Guidote, A. M.; Quirino, J. P. *Anal. Bioanal. Chem.* **2009**, *394*, 175-185.
(58) Slampova, A.; Mala, Z.; Gebauer, P.; Bocek, P. *Electrophoresis* **2017**, *38*, 20-32.
(59) Rappsilber, J.; Mann, M.; Ishihama, Y. *Nat. Protoc.* **2007**, *2*, 1896-1906.
(60) Kitigawa, F.; Kawai, T.; Otsuka, K. *Anal. Sci.* **2013**, *29*, 1129-1139.
(61) Kawai, T.; Watanabe, M.; Sueyoshi, K.; Kitagawa, F.; Otsuka, K. *J. Chromatogr.* **2012**, *1232*, 52-58.
(62) Martineau, M.; Shi, T.; Puyal, J.; Knolhoff, A. M.; Dulong, J.; Gasnier, B.; Klingauf, J.; Sweedler, J. V.; Jahn, R.; Mothet, J. P. *J. Neurosci.* **2013**, *33*, 3413-3423.
(63) Aerts, J. T.; Louis, K. R.; Crandall, S. R.; Govindaiah, G.; Cox, C. L.; Sweedler, J. V. *Anal. Chem.* **2014**, *86*, 3203-3208.
(64) Liu, J.-X.; Aerts, J. T.; Rubakhin, S. S.; Zhang, X.-X.; Sweedler, J. V. *Analyst* **2014**, *139*, 5835-5842.
(65) Lombard-Banek, C.; Moody, S. A.; Nemes, P. *Angew. Chem. Int. Ed.* **2016**, *55*, 2454-2458.
(66) Nemes, P.; Knolhoff, A. M.; Rubakhin, S. S.; Sweedler, J. V. *Anal. Chem.* **2011**, *83*, 6810-6817.
(67) Nemes, P.; Rubakhin, S. S.; Aerts, J. T.; Sweedler, J. V. *Nat. Protoc.* **2013**, *8*, 783-799.
(68) Onjiko, R. M.; Moody, S. A.; Nemes, P. *Proc. Natl. Acad. Sci. U. S. A.* **2015**, *112*, 6545-6550.
(69) Onjiko, R. M.; Portero, E. P.; Moody, S. A.; Nemes, P. *Anal. Chem.* **2017**, *89*, 7069-7076.
(70) Sun, L.; Zhu, G.; Yan, X.; Dovichi, N. J. *Curr. Opin. Chem. Biol.* **2013**, *17*, 795-800.
(71) Zhang, Z.; Sun, L.; Zhu, G.; Cox, O. F.; Huber, P. W.; Dovichi, N. J. *Anal. Chem.* **2016**, *88*, 877-882.

For TOC only

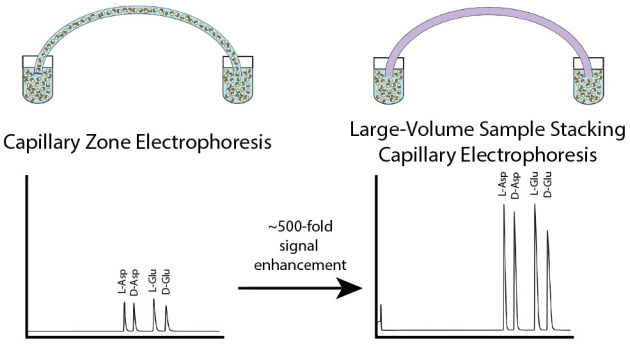
Capillary Zone Electrophoresis
Large-Volume Sample Stacking
Capillary Electrophoresis
~500-fold
signal
enhancement
L-Asp
D-Asp
L-Glu
D-Glu